DOI: 10.61782/fa.2025.0125

FORUM ACUSTICUM EURONOISE 2025

AN EXPERIMENTAL DATA SET FOCUSED ON METHODOLOGIES FOR THE *IN SITU* CHARACTERIZATION OF ACOUSTIC MATERIALS

João Vitor Pontalti[1*] **Eric Brandão**[1] **William D'Andrea Fonseca**[1]
Paulo Henrique Mareze [1] **Gustavo Netto**[1] **Efren Fernandez-Grande**[2]
[1] Acoustical Engineering, Federal University of Santa Maria (UFSM), Brazil
[2] Technical University of Madrid (UPM), Spain

ABSTRACT

The *in situ* characterization of acoustic materials is used to assess material properties of installed devices. The use of sensor arrays guarantees access to spatio-temporal information about the scattered sound field that finite samples or diffusers create in realistic conditions. Such effects can be investigated by formulating suitable inverse problems, which incorporates the complexity of acoustic fields. Since this line of research is in constant evolution, this paper describes the construction of a database of impulse responses obtained with *in situ* measurement techniques and some of the results obtained with different techniques. A 3D scanner is used to move and position the microphone at the coordinates of a pre-established array geometry. The exploited measurement scenarios, the data organization, and post-processing strategies are described. Initial results considering the classical 2-microphone method, plane-wave expansion and the discrete complex image source methods are presented and compared.

Keywords: *in situ measurements, absorption coefficient, dataset, acoustic materials*

1. INTRODUCTION

The acoustic characterization of materials under *in situ* or free-field conditions is valuable for room acoustics and noise-control applications. The work of Brandão [1] extensively reviews such techniques for measurement scenarios with a few sensors. Usually, these methods rely on a mathematical sound field model above the material and assume the sample to be much larger than the wavelength [2]. Additionally, microphone array techniques for absorption measurements have been explored since the early works of Tamura in the 1990s [3, 4], as they provide information about the distribution of pressure and/or particle velocity in space. Recent approaches that seek to evaluate the acoustical absorption coefficient have benefited from the use of microphone arrays in conjunction with inverse problem theories that aim to reconstruct the sound field in the vicinity of the sample under evaluation [5–11].

In order to promote further advancement in this research area, constructing a well-structured experimental dataset is of interest. For instance, some datasets reported in the literature focus on simulations for room acoustics [12], Head-Related Transfer Function simulations [13], and environmental acoustics [14]. This paper outlines the methodology adopted for creating a dataset of *in situ* measurements of acoustical materials.

The experiments described in this study were carried out in a large reverberation chamber using relatively low-cost instrumentation. A time-windowing technique was applied to isolate the direct sound from the reflections caused by the chamber walls. A 3D scanner is employed to move the microphone throughout the spatial coordinates of a pre-defined array, and impulse responses are collected sequentially. A more comprehensive overview of the experimental setup and the routines implemented in the construction of the dataset can be found in Ref. [15]. This study investigates a double planar array topology, as in Ref. [6, 16]. The measured sound pressure serves as

*Corresponding author: joao.pontalti@eac.ufsm.br.

input for two inverse problems: a plane wave expansion (PWE) [9] and a novel approach called the Discrete Complex Image Source Method (DCISM) [11]. The first can be used to study effects like edge diffraction of the sample, and the second is a compact sound field model suitable for short source-receiver distances. The inverse problems results are compared to those obtained with the classical two-microphone technique [17, 18].

This paper is organized as follows: Section 2 outlines the experimental procedures, encompassing the instrumentation built and used, the measured samples evaluated, and the array's geometries. Section 3 presents the mathematical background necessary to understand the inverse problems. Section 4 presents the results and discussions, followed by the conclusions in Sec 5.

2. MATERIALS AND METHODS

The experiments were conducted within a 207 m^3 reverberation chamber at the Acoustic Engineering Laboratory [19] of the Federal University of Santa Maria (UFSM - Brazil). The use of such a room was motivated by its controlled acoustic characteristics and by the fact that the walls can be substantially far from the sample and instrumentation [1]. The samples were positioned directly on the floor and in the center of the room. Figure 1b visually represents the experimental environment. This study presents results for 3 mounting conditions for 48×48 cm polyurethane (PU) foam with 25 mm of thickness. All evaluated scenarios consider the source positioned above the center of the sample at a distance of 1 m (normal incidence).

A 3D scanner, developed by the research team [10] was used to move a transducer through a set of predetermined spatial coordinates $\mathbf{r}_\mathrm{m} = (x, y, z)$. As the scanner operates, it sequentially measures the sound pressure at each coordinate. The scanner system, adapted from 3D printing technology, employs four NEMA stepper motors to move the microphone – two for the x axis (**M1** and **M2**), one for the y axis (**M3**), and another for z axis (**M4**) – providing three degrees of freedom. The scanner's control interface comprises an Arduino that handles the communication between the Python programming and the scanner, along with the drivers that operate the axis motors. A similar measurement system was envisioned and implemented by D'Antonio *et al.* [20]. Figure 1b illustrates the experimental setup mounted within the reverberation chamber, where it is possible to visualize the 3D scanner holding the microphone over the sample positioned directly below the sound source.

[1] Additionally, the laboratory does not have an anechoic room, unfortunately.

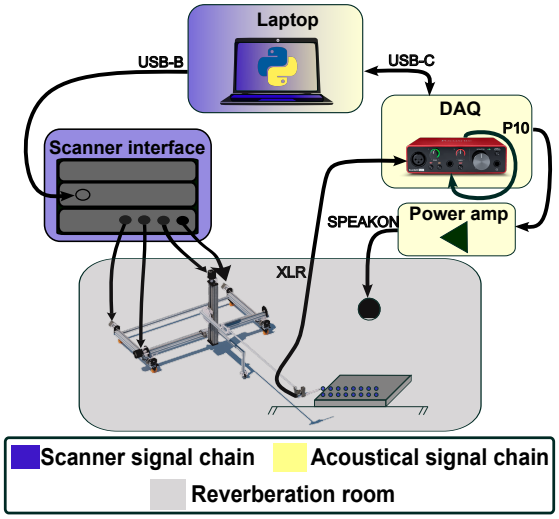

(a)

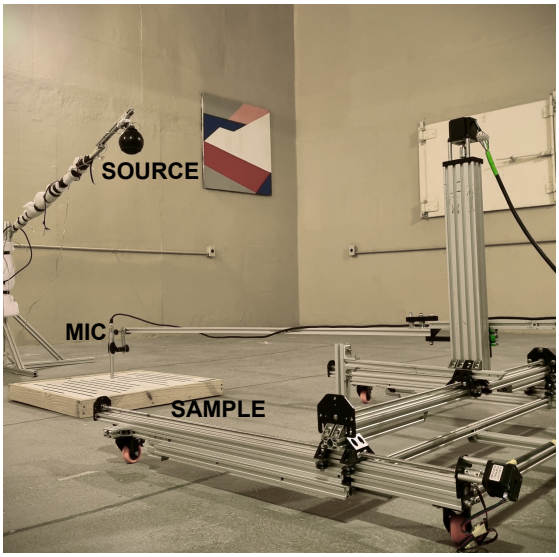

(b)

Figure 1: (a) Signal channeling with the cable connections. (b) Experimental setup within the reverberation chamber.

The acoustic signals reported herein were acquired using a Behringer ECM 8000 measurement microphone connected to a Focusrite Scarlett Solo audio interface

(ASIO driver). Other options were explored in the current dataset but are not reported here for the sake of brevity. The excitation signal consisted of an Exponential Sine Sweep (ESS) ranging from 100 Hz to 20 kHz, radiated from a full-range loudspeaker mounted on a spherical baffle with a diameter of 9 cm. A Brüel & Kjær 2716C power amplifier drives the loudspeaker. Both measurement and post-processing operate using Python, with object-oriented programming. The basic repositories primarily used in the work presented here are available on Github [21, 22]. Furthermore, the open-source library PyTTa Toolbox [23] was used extensively to create the excitation signals, record the responses, and compute the impulse responses. Atmospheric conditions, the name of the material under study, the hardware utilized, the Arduino setup, and the date and time of the measurements are stored as metadata on the measurement object and can be retrieved later.

The array explored in this paper is a double-layered microphone array, which evaluates the pressure above the sample's surface, $z > 0$. Its dimensions are 0.3×0.3 m^2, with 8 microphone positions along the x and y axis, resulting in 64 positions per layer and a total of $\mathcal{M} = 128$ measurement points. The vertical separation between the two layers was set to $\mathrm{z_r} = 0.02$ m, while the distance between the closest layer to the top of the sample was $\mathrm{z_0} = 0.02$ m.

3. THEORY OF INVERSE PROBLEMS

Many inverse problem formulations have been proposed over the years, aiming to reconstruct the sound field above finite or infinite samples. In this study, two approaches are considered: a plane wave expansion (PWE) model formulated as a set of propagating and evanescent plane waves [9] and the discrete complex image source method (DCISM), a novel method recently introduced in the literature by Brandao [11]. This paper briefly describes such methods, and more details can be found in the literature. In both cases, the inverse problem can be formulated as a matrix equation

$$\mathbf{p} = \mathbf{H}\mathbf{x} + \mathbf{n}\,, \tag{1}$$

where $\mathbf{p} \in \mathbb{C}^{\mathcal{M}}$ is the vector of measured sound pressures at $\mathrm{r_m}$, $\mathbf{x} \in \mathbb{C}^{l}$ contains the unknown amplitudes of interest, and $\mathbf{H} \in \mathbb{C}^{\mathcal{M}\mathrm{x}l}$ is the sensing matrix (Kernel), which models the acoustic field according to the method being implemented. Also, $\mathbf{n}$ is representative of noise that contaminates all measurements and model inconsistencies [6,9]. Typically, the dimensions of ℓ and $\mathcal{M}$ differ, and the inverse problem becomes ill-posed, requiring regularization. The main topics regarding the assembly of the sensing matrix for both PWE and DCISM are discussed in Secs. 3.1 and 3.2. Further notes on the reconstruction stage are given in Sec. 3.3.

3.1 Plane wave expansion

The basic formulation presented in this section if based on Refs. [6, 9]. It is assumed that the measured sound pressure can be represented as a superposition of ℓ propagating and evanescent plane waves, separated in an incident and a reflected sound field. Thus, the kernel matrix can be written as $\mathbf{H} = [\mathbf{H}_{\mathrm{inc}}, \mathbf{H}_{\mathrm{ref}}]$. For a given receiver at $\mathbf{r}_\mathrm{m} = (x, y, z)$ and a wave-number $\mathbf{k}_\ell$, the matrix elements are composed of

$$\begin{aligned} \psi_\ell^{\mathrm{inc}}\left(\mathbf{r}_\mathrm{m}\right) &= \mathrm{e}^{-\mathrm{j}\left(k_x x + k_y y + k_z\left(z - z^{+}\right)\right)}, \\ \psi_\ell^{\mathrm{ref}}\left(\mathbf{r}_\mathrm{m}\right) &= \mathrm{e}^{-\mathrm{j}\left(k_x x + k_y y - k_z\left(z - z^{-}\right)\right)}, \end{aligned} \tag{2}$$

with z^+ and z^- related to retracted virtual source planes that help to regularize the problem [6,9].

3.2 Discrete complex image source method

This formulation, proposed in Ref. [11] is based in Ref. [24]. It models the sound field as composed of a monopole (associated with the original source - incident sound field), a component associated with the image source, and a series of monopoles located along a complex line (reflected sound field). The matrix kernel is given by

$$G(\mathbf{r}_\mathrm{i}, \mathbf{r}_\mathrm{m}) = \frac{b}{2} w_\mathrm{i} \frac{\mathrm{e}^{-\mathrm{j}k|\mathbf{r}_\mathrm{i} - \mathbf{r}_\mathrm{m}|}}{|\mathbf{r}_\mathrm{i} - \mathbf{r}_\mathrm{m}|}\,. \tag{3}$$

For the original sound source, $\mathrm{i} = 1$, $\mathbf{r}_1 = (x_\mathrm{s}, y_\mathrm{s}, z_\mathrm{s})$. For the image source, $\mathrm{i} = 2$ and $\mathbf{r}_2 = (x_\mathrm{s}, y_\mathrm{s}, -z_\mathrm{s})$ ($\frac{b}{2} w_\mathrm{i} = 1$ in both cases). For the remaining complex sources $\mathrm{i} = 1, 2, \cdots, N$, $\mathbf{r}_\mathrm{i} = (x_\mathrm{s}, y_\mathrm{s}, -z_\mathrm{s} + \mathrm{j}q_\mathrm{i})$, with w_i and q_i given by the Gauss-Legendre quadrature rule, and b being a suitable truncation value for the integral [11, 24].

3.3 Inverse problem estimation and reconstruction

Given that the Kernel matrix $\mathbf{H}$ in Equation 1 leads to an ill-posed problem, an appropriate regularization technique is required to stabilize the inversion. This issue is addressed through Tikhonov regularization, which is formulated as

$$\tilde{\mathbf{x}} = \underset{\mathbf{x}}{\mathrm{argmin}} \left(\|\mathbf{H}\mathbf{x} - \mathbf{p}\|_2^2 + \lambda \|\mathbf{x}\|_2^2 \right), \tag{4}$$

with λ being the regularization parameter selected automatically by generalized cross-validation [25]. After finding $\tilde{\mathbf{x}}$, the sound pressure and the normal component of the particle velocity can be reconstructed over a set of K grid points located at the sample's surface. The reconstructed sound pressure is given by

$$\tilde{\mathbf{p}}_{\mathrm{re}} = \mathbf{H}_{\mathrm{re}}\tilde{\mathbf{x}}\,. \tag{5}$$

with $\tilde{\mathbf{p}}_{\mathrm{re}} \in \mathbb{C}^K$ being the reconstructed sound pressure vector and $\mathbf{H}_{\mathrm{re}} \in \mathbb{C}^{K\times\ell}$ the reconstruction matrix containing the wave functions evaluated at the reconstruction points. The particle velocity vector is retrieved by means of Euler's equation of motion, with $\tilde{\mathbf{u}}_{\mathrm{re}} = \frac{-1}{\mathrm{j}k\rho c}\nabla\mathbf{H}_{\mathrm{re}}\tilde{\mathbf{x}}$. Utilizing the reconstructed sound pressure and the particle velocity, an estimation of the surface impedance can be derived as either a point-wise impedance or the spatial average of a set of grid points used to compute the reconstructed surface impedance, where

$$\tilde{Z}_s\left(\mathbf{r}_s\right) = -\frac{1}{\rho c}\frac{\tilde{p}\left(\mathbf{r}_s\right)}{\tilde{u}_n\left(\mathbf{r}_s\right)}, \tag{6}$$

where ρ is the air density and c the sound velocity in the air. Subsequently, the sound absorption coefficient is inferred as

$$\alpha = 1 - \left|\frac{\bar{Z}_s\cos(\theta) - 1}{\bar{Z}_s\cos(\theta) + 1}\right|^2. \tag{7}$$

4. RESULTS

This section presents the main results and corresponding discussions from the experimental measurements. The acoustic sound field is analyzed in the wave number domain using the PWE introduced in Sec. 3.1, and the absorption coefficient is reconstructed using both proposed methodologies. For comparison purposes, the absorption coefficient (α) is also estimated using the conventional two-microphone technique [17] for each tested sample.

Three polyurethane (PU) foam configurations are evaluated: (i) a flat rectangular sample (25 mm thick); (ii) a corrugated sample with similar maximum thickness; and (iii) a composite configuration consisting of the corrugated foam mounted on the top of the flat sample.

The initial stage of the post-processing is the analysis of the impulse responses (IRs) and their corresponding frequency response functions (FRFs) to provide an initial assessment of the measurement quality. Figure 2 presents an IR obtained from the measurement of the flat PU foam,

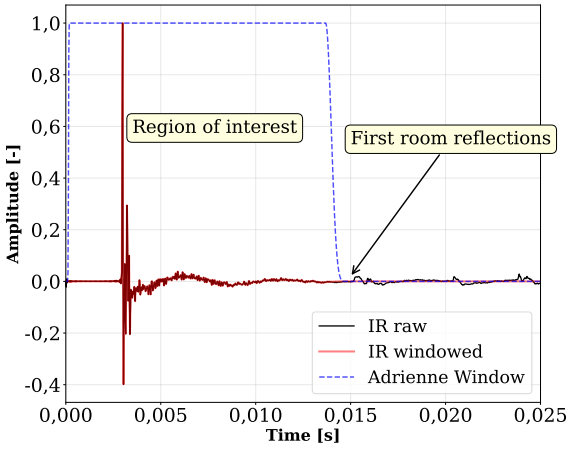

(a)

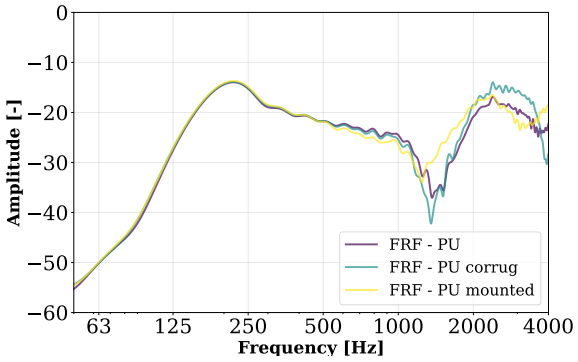

(b)

Figure 2: (a) Measured impulse response alongside its windowed version and the applied window function. (b) FRF obtained from one measurement of each sample.

showing both the raw and windowed impulse responses, as well as the Adrienne window applied to the signal. The first reflections from the chamber walls reach the transducer at approximately 0,015 s after the direct sound. It is important to note that this time delay can vary depending on the spatial positioning of the microphone within the reverberation chamber.

Furthermore, Figure 2b displays the FRFs (windowed signal) obtained from the first measurement of each sample (near its center). The difference between the samples

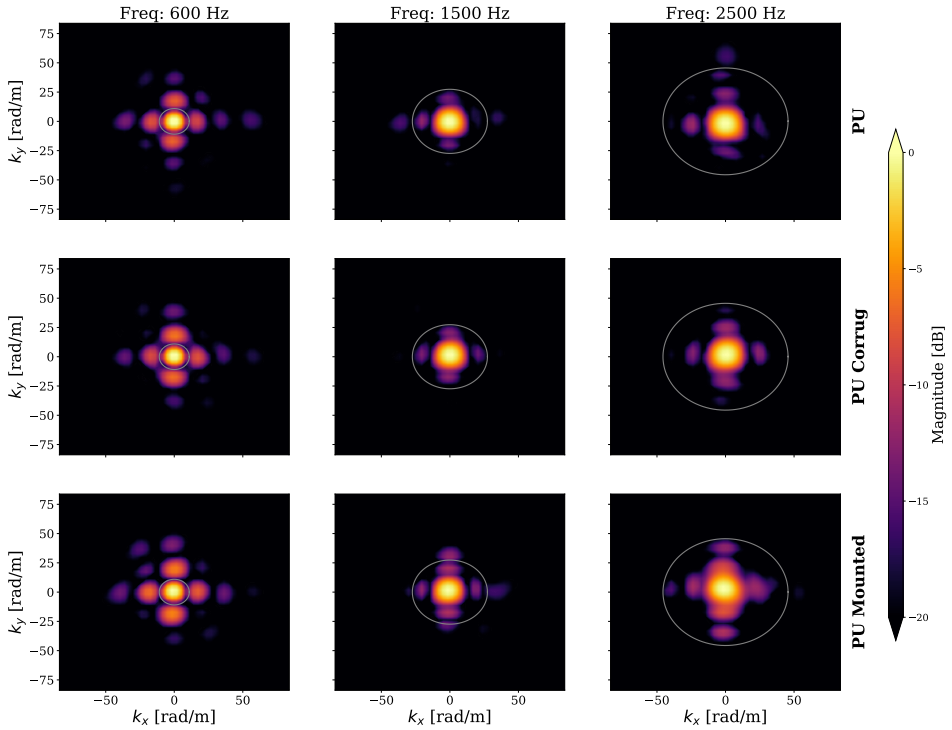

Figure 3: Wave-number spectrum for the PU sample estimated from the microphone array data.

is easier to be observed above 1000 Hz. Note that for the mounted sample, the magnitude of the FRF is significantly different than the others between 1 and 2 kHz.

Figure 3 shows the reflected components of the wave-number spectrum (k-space) at frequencies 500, 1500, and 2500 Hz for the PU flat, corrugated, and the mounted (corrugated + flat) situations. Each subfigure plots the radiation circle as a gray line to distinguish between propagating and evanescent plane waves. The source planes are located 1 cm below the lower layer of the microphone array and at 1 cm above the top layer. That ensures symmetry between the distances from the microphone array to the sample and to the source planes. In Fig. 3, the main lobe at the center of each subplot is associated with plane waves traveling in the direction of specular reflection, while the side lobes are likely due to the finite dimensions of the absorbers [9]. In all cases, at the frequency of 500 Hz, the wave-number spectra are similar and the evanescent components appear more prominent compared to the other spectra. This behavior is attributed to the fact that the wavelength of the incident wave is comparable to the size of the sample, which enhances the diffraction effects. The evanescent components tend to decrease in amplitude with increasing frequency, indicating a greater concentration of propagating waves at higher frequencies. It is interesting to note that the diffraction components for the corrugated samples seem to have slightly larger amplitudes when compared to the flat sample at 1500 and 2500 Hz, which can be attributed to a more irregular reflection pattern caused by the surface irregularities.

The absorption coefficient values for the three mounting configurations are shown in Fig. 4. The solid lines correspond to the results obtained using the DCISM method, while the dashed lines represent the values estimated using the PW approach. Dash-dotted lines are representative of the 2-mics technique. The three inference methods yield similar results across all configurations and mounting conditions. The DCISM and the plane-wave expansion methods show a closer agreement. Notably, the

DCISM tends to underestimate the absorption values below 500 Hz (compared to the plane-wave expansion). This discrepancy can be attributed to the different modeling assumptions. The absorption values for the stand-alone corrugated sample are relatively low because the average material thickness is small. For this reason, the estimates obtained using the two-microphone method show more erratic behavior above 1000 Hz. Note also that the absorption coefficient increases significantly for the mounted condition (corrugated on top of the flat sample). In both corrugated sample cases, it might be challenging to establish a surface to reconstruct the surface impedance on, which may contribute to the discrepancies between the DCISM and the plane-wave expansion models.

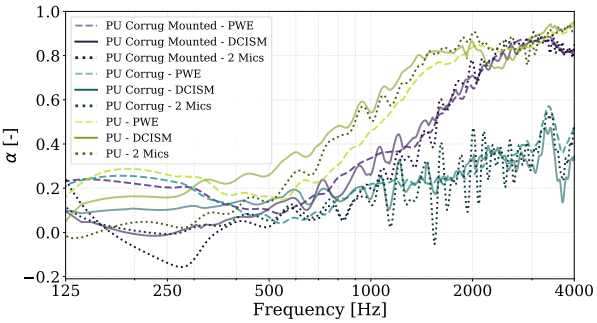

Figure 4: The sound absorption coefficient for 3 mounting conditions of finite PU samples measured with a double planar array.

5. CONCLUSIONS

The proposed experimental setup effectively measured impulse responses near three material configurations. The measurements performed with the double-layered array proved consistent, and the implemented inverse methods yielded satisfactory and insightful results regarding the behavior of the acoustic sound field. Additionally, both the PW method and the DCISM demonstrated consistency in reconstructing the absorption coefficient, with minor discrepancies aligned with predictions found in the literature. The two-microphone technique also proved to be a straightforward and reliable approach for establishing a a metric for comparison. The data presented herein will be included into the *in situ* acoustic database currently under development.

6. ACKNOWLEDGEMENTS

The authors would like to acknowledge the support and infrastructure of the Acoustic Engineering Department (EAC) at the Federal University of Santa Maria (UFSM), which made this work possible. This work is part of a research project into the spatial/temporal characterization of acoustic materials. The authors would like to thank the CNPQ universal project (No. 402633/2021-0) and PIBIC (Institutional Program for Scientific Initiation Scholarships) for their financial support.

7. REFERENCES

[1] E. Brandão, A. Lenzi, and S. Paul, "A review of the in situ impedance and sound absorption measurement techniques," *Acta Acustica united with Acustica*, vol. 101, no. 3, pp. 443–463(21), 2015.

[2] E. Zea, E. Brandao, M. Nolan, J. Cuenca, J. Andén, and U. Svensson, "Sound absorption estimation of finite porous samples with deep residual learning," 09 2023.

[3] M. Tamura, "Spatial fourier transform method of measuring reflection coefficients at oblique incidence. i: Theory and numerical examples," *The Journal of the Acoustical Society of America*, vol. 88, pp. 2259–2264, 11 1990.

[4] M. Tamura, J. Allard, and D. Lafarge, "Spatial fourier-transform method for measuring reflection coefficients at oblique incidence. ii. experimental results," *Journal of The Acoustical Society of America - J ACOUST SOC AMER*, vol. 97, pp. 2255–2262, 04 1995.

[5] M. Nolan, "Estimation of angle-dependent absorption coefficients from spatially distributed in situ measurements," *The Journal of the Acoustical Society of America*, vol. 147, pp. EL119–EL124, 02 2020.

[6] J. Hald, "Basic theory and properties of statistically optimized near-field acoustical holography," *The Journal of the Acoustical Society of America*, vol. 125, pp. 2105–2120, 04 2009.

[7] A. Richard and E. Fernandez-Grande, "Comparison of two microphone array geometries for surface impedance estimation," *The Journal of the Acoustical Society of America*, vol. 146, pp. 501–504, 07 2019.

[8] M. Alkmim, J. Cuenca, L. de Ryck, and W. Desmet, "Angle-dependent sound absorption estimation using a compact microphone array," *The Journal of the Acoustical Society of America*, vol. 150, pp. 2388–2400, 10 2021.

[9] E. Brandão and E. Fernandez-Grande, "Analysis of the sound field above finite absorbers in the wavenumber domain," *The Journal of the Acoustical Society of America*, vol. 151, no. 5, pp. 3019–3030, 2022.

[10] G. Souza, "Desenvolvimento de um escâner automatizado para medição sequencial e caracterização espaço-temporal de materiais acústicos." https://repositorio.ufsm.br/handle/1/27197, 2022.

[11] E. Brandão, W. D. Fonseca, P. H. Mareze, C. Resende, G. Azzuz, J. Pontalti, and E. Fernandez-Grande, "Sound absorption estimation using the discrete complex image source method and array processing," *Mechanical Systems and Signal Processing*, vol. 231, p. 112617, 2025.

[12] F. Brinkmann, L. Aspöck, D. Ackermann, R. Opdam, M. Vorländer, and S. Weinzierl, "A benchmark for room acoustical simulation. concept and database," *Applied Acoustics*, vol. 176, p. 107867, 2021.

[13] M. Marschall, J. G. Bolaños, S. T. Prepeliță, and V. Pulkki, "A database of near-field head-related transfer functions based on measurements with a laser spark source," *Applied Acoustics*, vol. 203, p. 109173, 2023.

[14] B. Gauvreau, "Long-term experimental database for environmental acoustics," *Applied Acoustics*, vol. 74, no. 7, pp. 958–967, 2013.

[15] J. V. Pontalti, E. Brandao, W. D'A. Fonseca, P. H. Mareze, and F. R. Mello, "Criação de um banco de dados de medições de materiais acústicos in situ," in *Actas del XIII Congreso Iberoamericano de Acústica FIA 2024*, (Santiago, Chile), pp. 867–877, Sociedad Chilena de Acústica (SOCHA), 2024.

[16] A. Richard and E. Fernandez-Grande, "Comparison of two microphone array geometries for surface impedance estimation," *The Journal of the Acoustical Society of America*, vol. 146, pp. 501–504, 07 2019.

[17] J. F. Allard and B. Sieben, "Meaurements of acoustic impedance in a free field with two microphones and a spectrum analyzer," *The Journal of the Acoustical Society of America*, vol. 77, no. 4, pp. 1617–1618, 1985.

[18] Y. Allard, J. F.; Champoux, "In situ two-microphone technique for the measurement of the acoustic surface impedance of materials," *Institute of Noise Control Engineering*, vol. 32, pp. 15–23, 1 1989.

[19] W. D'A. Fonseca, E. Brandão, P. H. Mareze, V. S. Melo, R. A. Tenenbaum, C. dos Santos, and D. X. da Paixão, "Acoustical engineering: a complete academic undergraduate program in Brazil," *The Journal of the Acoustical Society of America*, vol. 152, no. 2, pp. 1180–1191, 2022.

[20] P. D'Antonio, M. Nolan, and E. Fernandez Grande, "Design of a new sound field analysis recorder (sofar) for isotropy quantification in reverberation chambers," in *Proceedings of Inter-noise 2020*, (Lyon, France), 2020. 49¡sup¿th¡/sup¿ International Congress and Exposition on Noise Control Engineering, Inter-Noise 2020 ; Conference date: 23-08-2020 Through 26-08-2020.

[21] E. Brandão, "insitu_sim_python." https://github.com/eric-brandao/insitu_sim_python.

[22] E. Brandão, "scanner_meas." https://github.com/eric-brandao/scanner_meas.

[23] W. D'A. Fonseca, J. V. Paes, M. Lazarin, M. V. Reis, P. H. Mareze, and E. Brandao, "Pytta: Open source toolbox for acoustic measurement and signal processing," in *23rd International Congress on Acoustics - ICA 2019 (integrating 4th EAA Euroregio 2019)*, no. ISBN 978-3-939296-15-7, (Aachen, Alemanha), pp. 1–8, German Acoustical Society (DEGA), 2019.

[24] X. Di and K. E. Gilbert, "An exact laplace transform formulation for a point source above a ground surface," *The Journal of the Acoustical Society of America*, vol. 93, pp. 714–720, 02 1993.

[25] P. C. Hansen, *Discrete Inverse Problems*. Society for Industrial and Applied Mathematics, 2010.